Combined model predictive control and ANN-based forecasters for jointly acting renewable self-consumers: an environmental and economical evaluation

Simone Negri[a], Federico Giani[a], Nicola Blasuttigh[b], Alessandro Massi Pavan[b], Adel Mellit[c], Enrico Tironi[a]

[a] Department of Electronics, Information and Bioengineering, Politecnico di Milano, Italy
[b] Department of Engineering and Architecture, and Center for Energy, Environment and Transport Giacomo Ciamician - University of Trieste, Italy
[c] Department of Electronics, Renewable Energy Laboratory, University of Jijel, Algeria
E-mail addresses: simone.negri@polimi.it, federico.giani@mail.polimi.it, nicola.blasuttigh@phd.units.it, enrico.tironi@polimi.it, apavan@units.it, adelmellit2013@gmail.com

***Abstract*— Recent European Community directives introduce Renewable Energy Communities (REC) and Jointly Acting Renewable Self-Consumers (JARSC). Both entities are constituted by communities of residential and/or non-residential prosumers, located in proximity of renewable generators and Electrical Storage Systems (ESS) owned and managed by the REC/JARSCs. These aggregations of prosumers are aimed at providing environmental and economic benefits by maximizing their global self-consumption. In this frame, it is relevant to introduce a control strategy which considers the whole system represented by the REC/JARSCs and performs optimal management of energy production, storage and consumption. The present paper proposes a Model Predictive Control (MPC) based control design, targeted at the minimization of electricity cost and equivalent CO2 emissions, considering the whole ensemble of loads included in the REC/JARSCs over a 24-hours prediction horizon. To exploit the MPC ability of including forecasts in the optimization problem, predictors including Artificial Neural Networks (ANN) are developed for solar irradiance, air temperature, electricity price and carbon intensity. The proposed control performance is evaluated considering a case study located in Milan, Italy, and its advantages with respect to traditional control algorithms are highlighted by comprehensive numerical simulations. Lastly, an economic evaluation of the considered system is presented.**

Keywords—Model predictive control, neural networks, renewable energy communities, jointly acting renewable self consumers, electricity market, CO2 emissions.

1. Introduction

New scenarios are disclosing for electric power distribution systems and new opportunities are opening for consumers. The recent directives 2018/2001 [1] and 2019/944 [2] from European Community, which are currently undergoing the transposition process by Member States, are pushing towards an improvement in the valorisation of self-consumption of renewable energy generation, in particular photovoltaic (PV) and wind generation. The articles 21 and 22 of the RED II directive [1] introduce Renewable Self-Consumers (RSC), Jointly Acting Renewable Self-Consumers (JARSC) and Renewable Energy Communities (REC). RSCs, JARSCs and REC members, "individually or through aggregators, are entitled: (a) to generate renewable energy, including for their own consumption, store and sell their excess production of renewable electricity, including through renewables power purchase agreements, electricity suppliers and peer-to- peer trading arrangements […] (b) to install and operate electricity storage systems combined with installations generating renewable electricity for self- consumption […]; (c) to maintain their rights and obligations as final consumers; (d) to receive remuneration, including, where applicable, through support schemes, for the self-generated renewable electricity that they feed into the grid, which reflects the market value of that electricity and which may take into account its long-term value to the grid, the environment and society". The Member States are transposing the indication included in the European Directives in an heterogenous way, the tracking and discussion of which lies outside the purposes of this paper. However, the common factor which can be clearly identified is RSCs, JARSCs and RECs being a further instrument pushing the transformation of final consumers into groups of subjects (prosumers) capable of producing, consuming, storing and sharing electrical energy generated by means of renewable energy sources.

Another aspect of relevance, under the light of the recent policies towards decarbonization, is the evaluation of the equivalent emissions of CO2 generated by the electrical system [3]. At the moment, CO2 emissions are not included in electricity price for residential users, but, considering the relevance of decarbonization targets, it is of interest to consider how to limit CO2 emissions.

* Corresponding Author: Dr. Simone Negri, email: simone.negri@polimi.it, address: Politecnico di Milano, Dipartimento di Elettronica, Informazione e Bioingegneria, Via Ponzio 34/5, 20133 Milano Italia
Published version available, DOI 10.1016/j.renene.2022.07.065

It is hence relevant to introduce a control strategy which considers the whole system represented by the REC, JARSCs or RSCs and performs optimal management of energy production, storage and consumption. Consequently, energy flows can be optimized with the aim of maximizing self-consumption and power shared among the REC members or RSCs, which implies a reduction in cost through available incentive mechanisms, and lowering CO2 equivalent emissions.

RECs are extensively debated in the literature. Several authors have already analysed the REC and JARSC frameworks in order to provide a comprehensive overview of regulations and technical/economical assessments. For example, [4], [5] aim to review the regulatory frameworks among different EU member states showing that most of the countries have already developed tariffs definition to support REC although in some countries there is still no clear structure with different boundaries regarding REC definitions. In [6], a general overview of the REC and RSC is shown, by investigating different aspects regarding the integration of REC and the actual power system, also from the ancillary service and demand response perspectives. Moreover, several projects have already been developed around Europe demonstrating the considerable interest from governments, research institutes, private entities, and end users [7] - [9]. From the control and optimization aspect, [10] proposes smart metering and electric vehicles charging solutions to increase the self-consumption in a REC by regulating the EV charging power during the day while [11] has studied machine learning techniques to improve self-consumption on an existing wind-power REC in Belgium. A multi-agent approach is analysed in [12] where the coordination of a set of shiftable loads is optimized to maximize the self-consumption of a shared PV system in a JARSC building. Increases in self-sufficiency and self-consumption of up to 98% and 81% are obtained, as well as showing the differences between different control architectures. Naturally, the willingness of agents to participate in this strategy must be considered. In [13], an innovative power-sharing model is proposed both for JARSC and REC aiming to always make the end user passive towards the grid. In this way, only one dedicated point of connection is seen as active user. However, no storage has been considered and a real-time control is performed without any optimization method. Finally, in [14], [15] a procedure is proposed for the optimal design of electrical and thermal installations as a function of total costs and CO_2 emissions reduction. In addition to the economic aspect, although important from the point of view of the end user and the community, the environmental perspective plays a key role, especially in this context where the main aim of the incentive is also decarbonisation. In fact, more and more attention is also being paid to this aspect in view of a possible introduction of remuneration for the CO2 emissions avoided [16]. Although different works have been conducted regarding the joint optimisation between costs and carbon intensity in different energy entities with different optimisation techniques [17] - [21], no work has been found regarding the analysis of REC or JARSCs with a trade-off approach between the two aspects.

From a control perspective, REC and JARSCs represent a form of grid-connected microgrid, the control of which have been largely debated in literature in recent years. When optimal dispatchment of available resources is the main control task, Model Predictive Controllers (MPC) are often considered. Indeed, MPC controllers are particularly suited for microgrid control as they calculate control action as an optimization problem over a defined prediction horizon, which allows integrating available forecasts and constraints in control action calculations [22], [23]. Additionally, since the control action is calculated by means of a constrained optimization problem, MPC controllers are suited to manage different tasks with conflicting requirements [22], [23]. Indeed, some papers propose MPC-based controllers for microgrids [24] - [30], addressing different tasks spanning from voltage control to economic optimization and hierarchical control. In these regards, it is clear that the MPC control performances are related to forecasts reliability, and significant literature is available for PV generation, electricity price, carbon intensity and load [31] - [45]. For this tasks, ANN-based predictors proved to be a suitable solution for PV generation forecasts [31] - [33].

The present paper considers a case study located in Milan, Italy, and constituted by multi-apartment block, which classifies as a community of consumers connected to the public distribution network. The multi-apartment block includes twelve consumers and one set of common services, including PV generation and ESS. Consequently, the regulatory prescriptions considered are the Italian transposition of the referenced European Directives. For the management of available resources, this paper proposes a Model Predictive Control (MPC) based control design, targeted at the minimization of electricity cost and equivalent CO2 emissions, considering the whole ensemble of loads included in JARSCs over a 24-hours prediction horizon. To take maximum advantage from the MPC ability of including forecasts in the optimization problem, predictors including Artificial Neural Networks (ANN) are developed for solar irradiance, air temperature, electricity price and carbon intensity. The proposed control performance is evaluated by means of a comprehensive set of numerical simulation and its advantages with respect to traditional control algorithms are highlighted. The presented results highlight that the proposed MPC controller provides a significant improvement in electricity cost savings by maximizing self-consumption over the 24-hours prediction horizon. Additionally, the equivalent CO2 emissions are effectively reduced.

The paper is structured as follows: Section 2 reports the considered case study, including sizing and parameters of the main components, loads and generation profiles and control problem statement. Section 3 reports: a) the models used for system simulations, b) the MPC control design, including model selection and optimization problem formulation, and c) the definition of available forecasts, including statistical data and the proposed ANN-based predictor. The performed numerical simulations are detailed in Section 4, where numerical results are discussed and compared with a benchmark simulation including standard control algorithms in place of the proposed MPC control. Economic indicators for the considered system are also evaluated in this Section. Lastly, final conclusions emerging from simulation results are reported in Section 5.

2. SYSTEM DESCRIPTION

In this Section, the considered electrical system as well as the scope of this work are detailed. First, a general overview of the different components is presented, followed by a detailed description of the consumption and generation profiles. At the end, the target of the problem is detailed by defining the incentive features of the collective self-consumption framework. As mentioned, the considered system represents a case study located in Milan. Even though all the data used for sizing and simulations are obtained from online databases, it is necessary to define a geographical location to maintain consistency among correlated data (e.g. irradiance and temperature)

2.1. System Overview and Components Description

2.1.1. System Overview

The considered system of JARSCs is shown in Figure 1. It is assumed that JARSCs are located in a building in the centre of Milan and consists of twelve apartments, all inhabited by different types of dwellers and families. Each user/apartment has its own energy meter (UM), owned and managed by the DSO. A PV system is installed on the roof of the building, the energy production of which is measured by the production meter (PM). In order to maximize the self-consumption, an "all-in-one" ESS has been included in order to store the surplus PV energy produced in the hours of lower consumption and maximum PV generation for later discharge during periods with small or null PV generation. The ESS includes an inverter, interfacing the DC section with the AC grid and providing PV and/or ESS energy to the common loads, hence improving the total self-consumption. The energy exchanged with the grid is measured through the common utility meter (CM).

The ESS system aims to optimally handle the PV generation by performing the Maximum Power Point Tracking (MPPT) function and manage the charge/discharge battery operation, and includes a Battery Management System (BMS) for balancing the temperatures and the state of charge (SoC) of the battery pack. It is assumed that the power exchanged by the battery can be controlled by an external signal, which will be the output of the MPC control discussed in Section 3, and that SOC measures/estimation are available from the ESS.

2.1.2. Photovoltaic System

The PV system is designed in order to cover most of the energy consumption of the considered JARSCs. The total energy consumption of the considered JARSCs, detailed in Section 2.2, is equal to 40 MWh/year. Considering to cover the 85% of the annual energy consumption with the PV generation, and considering that in Milan the annual energy generation of PV systems is roughly 1100 kWh/kWp, the required PV installed power result in 30.9 kW. Since the PV system is the only source of energy present in the microgrid, monocrystalline technology is selected as a common commercial solution. The selected module specifications (manufacturer is unessential and undisclosed) are reported in Table 1. To reach the required installed power by means of the selected PC modules, it is possible to use 3 series-connected modules per string and 26 parallel-connected strings, resulting in a total of 78 installed modules, the power of which is equal to 31.2 kWp. Note that this sizing procedure is not optimal from the economic point of view, but it is meant to have enough PV generation to cover most of the JARSCs needs, in order to reduce CO2 emissions, which is one of the driving reasons for the introduction of REC and JARSCs.

2.1.3. Storage System

With the aim of increasing the building self-consumption, a lithium-ion phosphate storage system has been included in the system under analysis. The sizing of the ESS is based on the energy which should ideally be stored on each day of the year, calculated as the difference between PV production and loads energy consumption in daily hours. The sum of said energy over one year is then divided by the number of days of the year in which PV production is larger than loads energy consumption in daily hours, resulting in a starting ESS sizing equal to 63 kWh. The considered ESS is then realized by means of four commercially available modules, each one having a capacity of 15 kWh. In order to reduce the degradation during the lifetime, a maximum

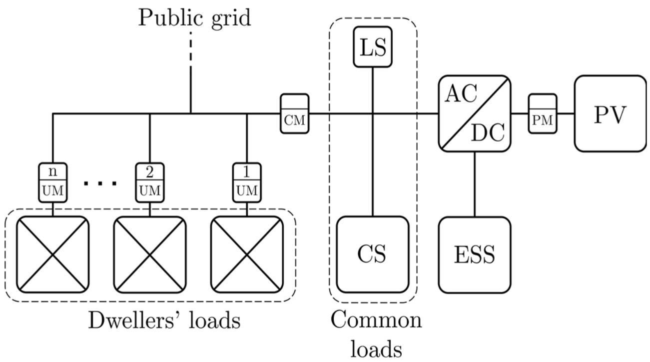

Figure 1. Considered system electrical schematic

TABLE 1 - PHOTOVOLTAIC MODULE TECHNICAL SPECIFICATION

Electrical Parameter at STC	Symbol	Value
Nominal Power	$P^{STC}_{md,M}$	400 W
Module Efficiency	η_{md}	22.6%
Rated Voltage	$V^{STC}_{md,M}$	65.8 V
Rated Current	$I^{STC}_{md,M}$	6.08 A
Open-Circuit Voltage	$V^{STC}_{md,OC}$	75.6 V
Short-Circuit Current	$I^{STC}_{md,SC}$	6.58 A

Temperature Coefficients	Symbol	Value
Current Temperature Coefficient	$\alpha^{\%}_{md,T}$	2.9 mA/°C
Voltage Temperature Coefficient	$\beta^{\%}_{md,T}$	-176.8 mV/°C
Power Temperature Coefficient	$\gamma^{\%}_{md,T}$	-0.29 % /°C

TABLE 2 - BATTERY MODULE SPECIFICATIONS

Electrical Data	Value
Rated module capacity	300 Ah
Efficiency	95 %
Rated Voltage	50 V
Rated C-rate	1 C
Depth of Discharge	90 %
Warranty	10 years
Battery Service Life	designed for over 20 years
Cycles	10000

Depth-of-Discharge (DoD) has been set in the simulations to comply with the manufacturer specifications. The main parameters of the battery module are listed in Table 2.

2.2. Load and Generation Profiles

2.2.1. Consumers Load Profiles

As mentioned, the multi-apartment block under investigation consists of twelve apartments, each inhabited by different occupants with different habits. In fact, with the aim of making the evaluation as faithful as possible, a wide spectrum of dwellers with different habits (and, therefore, different load profiles) has been considered. For this purpose, the Load Profile Generator (LPG) simulation tool [46] has been used, which allows automatic generation of residential electrical and water consumption based on psychological and behavioural profiles of the residents and possible daily activities which can be performed. A list of example consumption profiles is available at [47], the first twelve of which are used as load profiles in this paper. The list of the inhabitant's profiles, the corresponding amount of electricity consumption and their contractual power are shown in Table 3. In addition, Figure 2 shows the twelve load profiles corresponding to each apartment over one example week throughout the year. One can note that each profile has different properties depending on the presence of inhabitants, possible vacation periods and working hours. This not only makes it possible to correctly evaluate the economic and energy analysis of the problem, but also provides important characteristics on the periods of greatest consumption.

2.2.2. Common Load Profile

In multi-flat buildings, there is always a certain amount of electrical load needed for common services, the costs of which are usually divided among the inhabitants according to private agreements, which will not be discussed in this paper. The most common loads representing common services are the lighting of shared areas (courtyard, stairs, entrance) and lifters. Consequently, in absence of available data, an energy profile based on statistical considerations was created for lighting and elevators. With regard to lighting, a number of LED bulbs with an average power of 100 W were assumed. Absorption takes place over two time slots: between 5 a.m. and 9 a.m. and between 5 p.m. and midnight. During these time intervals, LED lighting is assumed to absorb, in each 5-minute interval, an instantaneous power between 50 W and 150 W, with gaussian distribution and average value equal to 100 W. Concerning the lift, [48] presented a study on different types of lifts highlighting that a significant power consumption generated by residential lifts is caused by the stand-by mode rather than by individual rides. In our model, according to measures presented in [48], an average stand-by power of 250 W was considered. Additionally, with regard to consumption in the running phase, an energy of 50 Wh per single run was assumed. The operating intervals are the same as for lighting with the addition of a lunchtime interval between noon and 2pm. Considering the total number of inhabitants in the building, from 6 to 18 runs for the morning and evening intervals and from 3 to 9 runs for the mid-day interval were considered, with random (gaussian) variations around the average value.

In addition to lifters and lighting, the increase in electric car purchases in recent years has also seen an increase in residential charging stations (wallboxes) as an additional common service for the inhabitants. For this reason, real energy profiles of a 22 kW

TABLE 3 – INHABITANTS DETAILS AND ELECTRICITY CONSUMPTION OVER ONE YEAR

Type	Electricity Consumption [kWh/year]	Contractual Power [kW]	Type	Electricity Consumption [kWh/year]	Contractual Power [kW]
Couple (F23-M25) both at work	2623	3.5	Single with work (M23)	1454	3.5
Couple (F37-M38), with work	1706	3.5	Single woman (F30) with work, two children (M11-M7)	3227	3.5
Family (F40-M43), single child (M10), both at work	2613	4	Single woman (F34) with work	1733	3
Couple (F45-M50), one at work, one at home	2870	5	Single man (M40) shift worker	2035	4
Family (F35-M40), three children (M13-M6-F4), both with work	4001	5	Female (F23) student	1563	3
Jobless (M30)	1265	3.5	Male (M22) student	1102	3

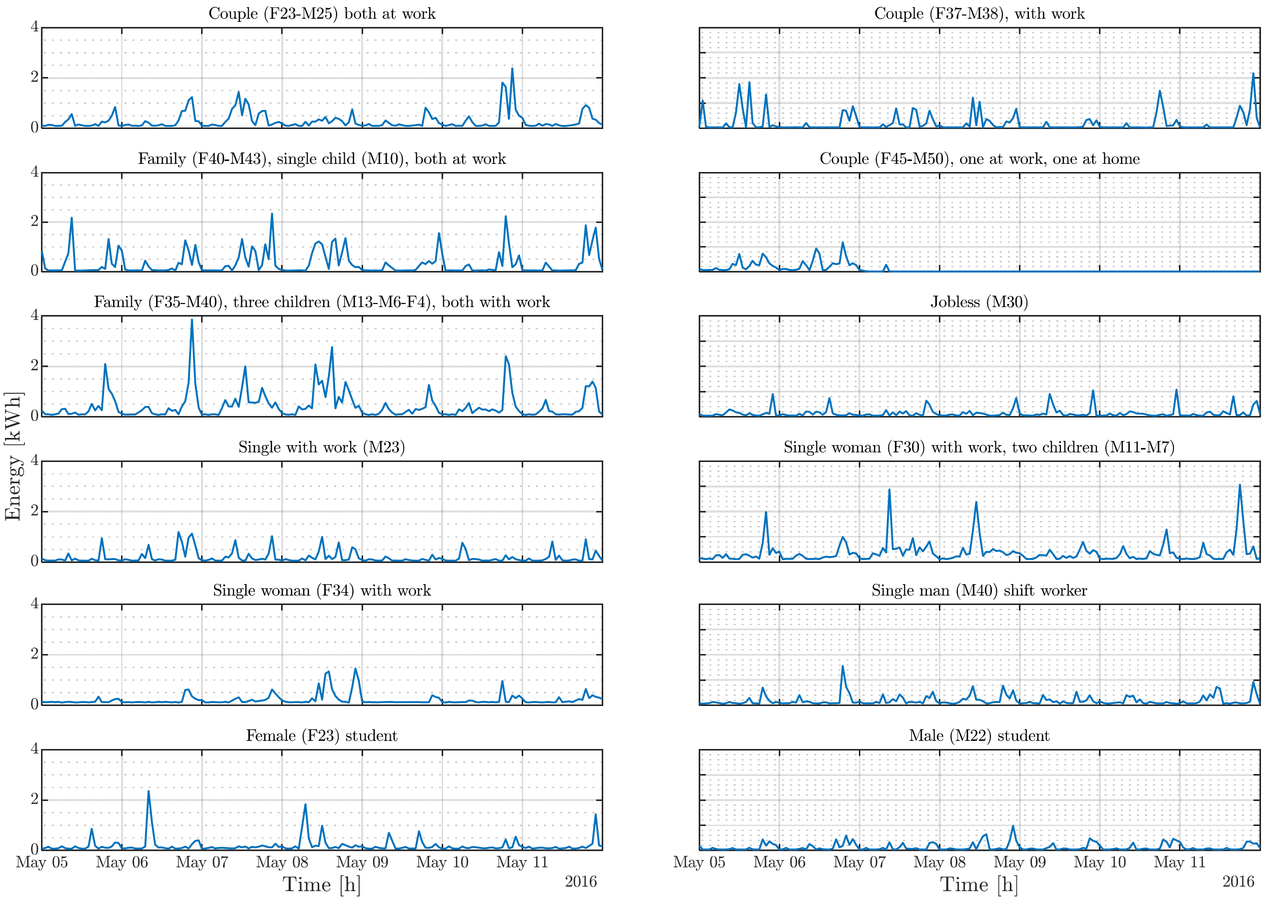

Figure 2. Example of electrical load profiles of the twelve apartments over one week

wallbox for residential use were considered for the charging of two 50 kWh electric vehicles. The two owners mainly use the vehicle for commuting, so that it is charged during the evening/night hours in order to have it fully charged the next morning. Charging is not externally controlled and the power profile is managed by the EV's internal BMS.

2.2.3. Photovoltaic generation profiles

Considering now solar irradiance and air temperature, statistical data are available online, provided by the Photovoltaic Geographical Information System (PVGIS), an online database managed by the European Science Hub [49]. This database provides both hourly profiles for complete years and aggregated data, such as monthly average radiation. Photovoltaic generation can be calculated as a function of solar irradiance and air temperature considering the expressions reported in [30]. Considering that the purpose of this paper is the design of an MPC controller, it is clear that also some forecasts of solar irradiance and air temperature would be of help. In these regards, the aggregated data (e.g. average daily profiles per month) available from PVGIS may be considered as a starting point for PV generation prediction. Further discuss on how to integrate statistical data in forecasts are reported in Section 3.4. The data used in this paper are referred to 2016, being it the most recent year for which all data are available for the considered location.

2.2.4. Electricity Price and equivalent carbon intensity profiles

Being minimization of cost and equivalent CO2 emissions the target of this paper, it is necessary to recall data about those quantities. Considering selling price, it is worth considering that, in Italy, two possibilities are considered. In fact, the surplus of energy production which is not directly consumed or stored to the battery is sold to the public grid. In Italy there are two types of procedures for selling energy to the grid. The first consists of payment by the distributor of a fixed minimum price (PMG - Prezzo Minimo Garantito). The second one consists of payment of energy through the real-time pricing (PO - Prezzo Orario), which varies hourly based on the energy markets and the electricity zone considered. In this study, we assume that the sale of energy is performed via PO, thus taking advantage of the variability of market prices. In these regards, PO values for the year 2016 in the ITA-NORTH electricity zone were extracted from the database of the European Network of Transmission System Operators for Electricity (ENTSO-E) [50]. Regarding the purchase cost, a variable cost was assumed based on the hourly zonal price by considering a possible implementation of a real-time pricing (RTP) type market that varies based on the needs of the distributor.

System charges, network services, excise taxes, trader's earnings and VAT were added to the PO at typical values for residential customers.

In addition to economic cost, buying energy from the grid does also imply an environmental cost in terms of CO2 emission. The energy produced carries a carbon dioxide content that depends on the energy mix of the country of production (and neighbouring countries, due to international energy exchange): the carbon intensity [gCO2eq/kWh] is the parameter that allows us to assess this aspect. This value changes considerably within the day hour by hour depending on how much energy is produced from renewable sources compared to production from fossil fuels. Therefore, it is possible to optimize the purchase of energy from the grid, reducing absorption during high-carbon intensity periods (night-time) and increasing absorption during low-carbon hours (daytime). Based on the types of production plants, their emission factors and amount of energy produced, it is possible to calculate the carbon intensity of the electricity of the specific area. The ENTSO-E platform provides the values and types of production on an hourly basis while the emission factors were extracted from the study in [51].

2.3. Incentive Plan for Shared Energy

As mentioned, recent directives from European Community require Member States to promote forms of self-consumption, including jointly acting self-consumption. From here on, we will refer to the Italian case, assuming that, even if other transposition of the European Directives may be technically different, the common idea driving this incentive system will produce comparable results. Even though detailed discussion on energy pricing will be presented in Sections 3 and 4 as part of the optimization problem formulation, this subsection aims to describe the operation of the incentive mechanism that should act as a lever for the promotion of REC and RSC. In principle, two different regulation models, namely physical and virtual [52], are possible. However, at present regulation refers only to the virtual one, where the participants in REC or JARSCs share energy by taking advantage of the Distribution System Operator (DSO) existing distribution grid. In this configuration, each inhabitant is connected through its own connection point (meter), as shown in Figure 1. The electricity system operator GSE (Gestore Sistema Energetico), in order to promote REC/RSCs, rewards local self-consumption by providing an economic incentive. The latter is calculated on the so-called "shared energy", which is equal to the hourly minimum between the electricity produced and fed into the grid by renewable sources and the electricity consumed by the set of subjects belonging to the REC or by RSCs. Shared energy is rewarded with: a) a compensation due to avoided grid losses and distribution charges of about 11.5 €/MWh and b) an incentive of 100 €/MWh for groups of JARSCs, 110 €/MWh for REC. In addition, since the energy produced is actually fed into the grid (virtual exchange), said energy is remunerated according to the electricity market. In this case, the common loads are connected upstream of the condominium meter, directly absorbing the PV energy and representing an additional form of self-consumption, which will need to be considered for economic analysis.

3. SYSTEM MODELLING AND CONTROL DESIGN

In this Section, the main systems models and forecasts used for the simulations described in Section 4 are presented. As far as the MPC controller is concerned, efficient solvers are available commercially (e.g. Gurobi [53], Cplex [54], etc.), along with specific MATLAB expansions (e.g. Yalmip [55]) to interface standard MATLAB code with the aforementioned commercial solvers. A consequence, the realization of an MPC controller requires a suitable system model, constraints and cost function, leaving the real problem solution and related issues to specific software. The system model is described in Section 3.2, while the optimization problem formulation is presented in Section 3.3. The data and forecasts used for simulation and provided to the MPC controller are detailed in Section 3.4.

3.1. System Model for Simulation Purposes

3.1.1. Electronic Power Converter

The considered system includes one converter interfacing PV and ESS to the public distribution system. For the purposes of this paper, the system is considered in quasi-stationary conditions, such that a detailed model of power converters and their control is not required. Consequently, they will be modelled as ideal converters with known efficiency (battery efficiency 95%, PV to grid efficiency 98%).

3.1.2. PV System Modelling

For the purposes of this paper, the PV modules can be simply modelled by means of their I-V characteristic, which allows determining the maximum power point as a function of ambient temperature and solar irradiance. The exact equations used in this paper can be found in [30].

3.1.3. ESS Modelling

Considering the target of this paper, an advanced battery model is not needed. The only characteristics which is necessary to model are those related with energy balance, namely State of Charge (SoC) and efficiency. Considering a constant efficiency η_{batt}, and assuming the ESS exchange power P_{batt} positive if drained, the energy exchanged by the ESS over one discrete time step Δt can be evaluated by means of:

$$E_{batt} = \left(\frac{1+\mathrm{sgn}(P_{batt})}{2} \frac{1}{\eta_{batt}} - \frac{1-\mathrm{sgn}(P_{batt})}{2} \eta_{batt} \right) P_{batt} \Delta t \qquad (1)$$

The ESS SoC variation over one discrete time step Δt can then be evaluated by means of

$$SoC(k) = SoC(k-1) - \frac{E_{batt}}{C_{batt}} \qquad (2)$$

where C_{batt} is the nominal ESS energy capacity.

3.2. *System Model for MPC Control Design*

The desired discrete-time system model is expressed in general form as:

$$\mathbf{x}(k+1) = \mathbf{A}\mathbf{x}(k) + \mathbf{B}\mathbf{u}(k) \qquad (3)$$

where **x**, **u** are, respectively, the state and input vectors and **A**, **B** are, respectively, the state and input matrices. In the considered case study, the only model required is a model of the storage devices SoC, which, combining (1), (2) can be formulated as:

$$SOC(k+1) = SOC(k) - \frac{\Delta t}{C_{batt}} \left(\frac{1+\mathrm{sgn}\left(P_{batt}(k)\right)}{2} \frac{1}{\eta_{batt}} - \frac{1-\mathrm{sgn}\left(P_{batt}(k)\right)}{2} \eta_{batt} \right) P_{batt}(k) \qquad (4)$$

Reformulating (4) in terms of states and inputs leads to:

$$x(k+1) = x(k) - \frac{\Delta t}{C_{batt}} u(k) \qquad (5)$$

Where $x(k) = SoC(k)$. The control u is defined as

$$u(k) = \left(\frac{1+\mathrm{sgn}\left(P_{batt}(k)\right)}{2} \frac{1}{\eta_{batt}} - \frac{1-\mathrm{sgn}\left(P_{batt}(k)\right)}{2} \eta_{batt} \right) P_{batt}(k) \qquad (6)$$

such that the control input u represents a virtual power exchanged with the battery, including efficiency. This allows to use a linear system model (5), to include constraint on battery power P_{batt}, and to map the non-linearity related to battery efficiency (6) as a constraint in the optimization problem in a computationally efficient way.

3.3. *Optimization Problem Formulation*

3.3.1. *Variables*

The proposed MPC controller is based on a quite simple model, as detailed in Section 3.2. However, since it is intended for minimizing costs and CO2 emissions, it will need to deal with quite a complex cost functions and constraints set. In order to make the problem formulation as clear as possible, a number of auxiliary variables are introduced.

Firstly, a set of continuous variables is necessary to represent the system operating point (X_0), states (**X**), and inputs (**U**). Note that the homologous variables appearing in Section 3.2 (*x, u*), indicated with lowercase letters, are referring to a single time step, while variables indicated as bold capital letters (**X**, **U**) are vectors representing variables over the prediction horizon. Successively, the following variables are defined:

- non-controllable exchanged energy $\mathbf{E}_{nc\,[13xN]}$: each column of $\mathbf{E}_{nc}$ is constituted by the energy absorbed, at one of the N steps of the prediction horizon, by the 13 connection points reported in Figure 1 when battery power P_{batt} is null. The first twelve elements of each column represent consumers' absorptions, and hence are strictly positive. The last element of each column includes common loads and PV generation, so that can be negative when PV generation is larger than common load. At each step, the first column of $\mathbf{E}_{nc}$ is built with real-time measures, while the subsequent N – 1 columns are built with forecast data.
- selling price, buying price and CO2 equivalent emission vectors $\mathbf{P}_{sell\,[1xN]}$, $\mathbf{P}_{buy\,[1xN]}$, $\mathbf{CO2}_{[1xN]}$: represent the evolution of selling price, buying price and carbon intensity, respectively, over the N steps in the prediction horizon. Similarly to matrix $\mathbf{E}_{nc}$, the first element of these vector represents a real-time measure, while the following ones are obtained from forecast data.
- battery exchanged power $\mathbf{P}_{ESS\,[1xN]}$: control variable over the prediction horizon, related to the system input **U** by means of (6) , introduced as a constraint (further details in Section 3.3.2). Battery exchanged power $\mathbf{P}_{ESS}$ is the optimization variable which

constitutes the output of the proposed MPC controller, and the first element of $\mathbf{P}_{\mathrm{ESS}}$ is used as control signal P_{batt} for the ESS and system simulation.

- PV generated power $\mathbf{P}_{PV\,[1\mathrm{x}N]}$: PV generated power over the prediction horizon. Note that the energy produced by the PV over the prediction horizon is included in $\mathbf{E}_{nc}$, but the PV generated power $\mathbf{P}_{PV}$ is required to define operational constraints.
- exchanged energy $\mathbf{E}_{[13\mathrm{x}N]}$: includes the battery exchanged power in energy balance. The first twelve elements of each column are equal to their counterparts in $\mathbf{E}_{\mathrm{nc}}$, while the last element is obtained as:

$$\mathbf{E}(13,k) = \mathbf{E}_{nc}(13,k) - P_{ESS}(k)\Delta t, \quad k \in [1,N] \quad (7)$$

- shared energy $\mathbf{E}_{shared\,[1\mathrm{x}N]}$: energy shared over the prediction horizon, as defined in Section 2.3. Considering that the energy injected into the grid by the PV/ESS node is identified, for each k-th step of the prediction horizon, as -$\mathbf{E}$(13,k), each element of $\mathbf{E}_{shared}$ is defined as

$$\mathbf{E}_{shared}(k) = \begin{cases} \min\left(\sum_{i=1}^{12}\mathbf{E}(i,k),\ -\mathbf{E}(13,k)\right) & if\ -\mathbf{E}(13,k) > 0 \\ 0 & if\ -\mathbf{E}(13,k) \le 0 \end{cases}, \quad k \in [1,N] \quad (8)$$

- sold energy $\mathbf{E}_{sold\,[1\mathrm{x}N]}$: energy sold over the prediction horizon, defined as

$$\mathbf{E}_{sold}(k) = \begin{cases} -\mathbf{E}(13,k) - \mathbf{E}_{shared}(k) & if\ -\mathbf{E}(13,k) > \mathbf{E}_{shared}(k) \\ 0 & if\ -\mathbf{E}(13,k) \le \mathbf{E}_{shared}(k) \end{cases}, \quad k \in [1,N] \quad (9)$$

- cost matrix $\mathbf{C}_{[13\mathrm{x}N]}$: defines the energy cost over the prediction horizon. The first twelve elements of each column, being residential users, are defined as:

$$\mathbf{C}(i,k) = VAT\left(C_{fix}(i) + \mathbf{E}(i,k)\mathbf{P}_{buy}(k)\right), \quad i \in [1,12],\ k \in [1,N] \quad (10)$$

where $C_{fix}(i)$ represents the portion of yearly fixed cost of the i-th users associated with each hour of the year and VAT is a coefficient including the value added tax. The last element of each column is quite more complex to be defined, as the PV/ESS node can both buy or sell energy. This results in

$$\mathbf{C}(13,k) = \begin{cases} VAT\left(C_{fix}(13) + \mathbf{E}(13,k)\mathbf{P}_{buy}(k)\right) & if\ \mathbf{E}(13,k) \ge 0 \\ VAT\,C_{fix}(13) - \mathbf{E}_{shared}(k)\left(\mathbf{P}_{sell}(k) + Inc\right) - \mathbf{E}_{sold}(k)\mathbf{P}_{sell}(k) & if\ \mathbf{E}(13,k) < 0 \end{cases}, \quad k \in [1,N] \quad (11)$$

- CO2 total emission vector $\mathbf{CO2}_{total[13\mathrm{x}N]}$: defines the total CO2 emissions over the prediction horizon, defined as

$$\mathbf{CO2}_{total}(k) = \begin{cases} \mathbf{CO2}(k)\sum_{i=1}^{13}\mathbf{E}(i,k) & if\ \sum_{i=1}^{13}\mathbf{E}(i,k) > 0 \\ 0 & if\ \sum_{i=1}^{13}\mathbf{E}(i,k) \le 0 \end{cases}, \ k \in [1,N] \quad (12)$$

3.3.2. Constraints

In the following section, the optimization problem constraints are presented, which are:

- initial operating point: state variables must be equal to the measured battery SoC $x(k)$ related to the current time instant, according to

$$\mathbf{X}_0 = x(k) \quad (13)$$

- storage SoC is to be limited according to device capacity and DOD provided by the manufacturer, resulting in:

$$1 - DOD \le \mathbf{X} \le 1 \quad (14)$$

- the vector of control variables over the prediction horizon $\mathbf{U}$ can be represented, according to (6) as:

$$\mathbf{U}(k)=\left(\frac{1+\operatorname{sgn}\left(\mathbf{P}_{ESS}(k)\right)}{2}\frac{1}{\eta_{batt}}-\frac{1-\operatorname{sgn}\left(\mathbf{P}_{ESS}(k)\right)}{2}\eta_{batt}\right)\mathbf{P}_{ESS}(k)\text{ , k}\in[1,N] \qquad (15)$$

- battery exchanged power $\mathbf{P}_{\mathrm{ESS}}$ is to be limited according to converter capability and ESS C-discharge rating , resulting in:

$$-P_{\max C}\le\mathbf{P}_{ESS}\le P_{\max D} \qquad (16)$$

  where $\mathrm{P}_{\max C}$ is the maximum charge power and $\mathrm{P}_{\max D}$ is the maximum discharge power.

- it may be useful to consider the possibility of imposing the MPC controller not to buy energy from the grid to charge the battery, regardless of the possible economic convenience of this operation. In the said case, battery exchanged power $\mathbf{P}_{\mathrm{ESS}}$ is to be limited with respect to the PV generated power, resulting in:

$$\mathbf{P}_{ESS}\ge-\mathbf{P}_{PV} \qquad (17)$$

  the implications of this additional constraints will be discussed in Section 4.

3.3.3. Cost Function

The cost function to be used for optimization must consider, as mentioned, electricity cost and equivalent CO2 emissions. Consequently, the following quantities are defined:

$$J_{Cost}=\sum_{k=1}^{N}\sum_{i=1}^{13}\mathbf{C}(i,k) \qquad (18)$$

$$J_{CO2}=\sum_{k=1}^{N}\mathbf{CO2}_{total}(k) \qquad (19)$$

where J_{Cost} represents the total electricity cost over the prediction horizon as a function of the optimization variable P_{ESS}, while J_{CO2} represents the total equivalent CO2 emissions over the prediction horizon as a function of the optimization variable P_{ESS}. In addition to these costs, it may be of interest to introduce a further cost term to avoid possible issues related to inconsistencies in forecasts. This additional term is defined as:

$$J_{prev}=\begin{cases}-\left(1-\mathbf{X}(2)\right)\sum_{i=1}^{13}\mathbf{E}(i,1) & \text{if } \sum_{i=1}^{13}\mathbf{E}(i,1)<0\\ 0 & \text{if } \sum_{i=1}^{13}\mathbf{E}(i,1)\ge 0\end{cases} \qquad (20)$$

This term is meant to associate an additional cost to energy sold while the battery is not fully charged. In fact, the summation in (20) represents the energy sold in the first step of the prediction horizon, while the term (1-**X**(2)) is null when the MPC foresee the battery to be fully charged on the second step of the prediction horizon. The effect of this additional cost on MPC behavior will be discussed in Section 4.

Defined the single terms (18) - (20), the desired cost function is defined as:

$$J=\alpha J_{Cost}+\beta J_{CO2}+\gamma J_{prev} \qquad (21)$$

where α, β, γ are coefficients used to assess the different priorities in the optimization process. In particular, α, β are chosen such that $\alpha\ge 0$, $\beta\ge 0$, with $\alpha+\beta=1$, in order to assess the priority of cost vs CO2 minimization. The term γ, on the contrary, is chosen equal to 1 if the additional cost (20) is desired to be considered in the optimization problem, null otherwise.

3.4. Available Data and Forecasts

As mentioned, one of the main strengths of MPC controllers is their ability to exploit available forecasts to optimize control action over the prediction horizon, and obviously the better performances are obtained when the available forecasts are accurate and reliable. Consequently, it is necessary to clarify which data are to be considered as available forecasts for the MPC controller, hence known a priori over the whole prediction horizon, and which ones are to be considered as measured data to be used in system simulation, hence known only in the simulation present and past steps.

3.4.1. Statistical Prediction of Solar Irradiance, Air Temperature Price and CO2 emissions and Loads

As mentioned in Section 2.2.3, the PVGIS database [49] provides average daily irradiation and temperature profiles on hourly base for each month of the year. Additionally, it provides daily irradiation and temperature profiles on hourly base for each day of the year. In this paper, the average daily profiles of each month have been considered as known and used as available forecast, both for irradiation and temperature, assuming the forecasts of each day of the month to be the same. Analogously, the daily irradiation and temperature profiles of each day has been used as measured data, not known a priori.

As reported in Section 2.2.4, hourly price and carbon intensity forecasts are available from online databases. Aggregated data, similar to the ones available for temperature and irradiance, are not available. Consequently, similar profiles are obtained, for a single day of each month, by averaging the available data of that month, hour by hour, both for price and carbon intensity. This allows using the same approach used for irradiance and temperature, in that the averaged data are used as known statistical predictions, while the original hourly profiles are used as measured data. Lastly, the same approach is applied to load profiles, both users' absorptions and common services absorption, as presented in Section 2.2.1 and 2.2.2. Averaged profiles are generated and used as known forecast data, while original hourly profiles are used as measured data

This approach provides long-term predictions with low effort, but it is not very accurate, in that solar irradiance and load absorption in particular are known to be subject to large variations with respect to its average value. For this reason, it is suitable for long-term predictions, where large deviations from the average trend and less likely. For the same reasons, this approach is less suitable for short-term predictions, where irradiance and load variations may be significant and produce more significant effect on system operation. Consequently, a more effective solution for short-term prediction is introduced in Section 3.4.2.

3.4.2. ANN-based Prediction of Solar Irradiance, Air Temperature Price and CO2 emission

As mentioned, the availability of reliable prediction is a key factor for the development of an efficient MPC controller. In these regards, it is of interest to consider machine learning techniques for this task. It is worth considering that, ideally, not only reliable predictions are desired, but the predictor also needs to be as simple as possible to be compatible with real-time applications with no need for expensive high-performance processors. For these reasons, the well-known Feed-Forward Neural Network (FFNN) [56] has been selected to predict both solar irradiance (G) and air temperature (T). Even though FNNNs represent the simplest form of artificial neural networks, their ability to solve complex problems by mapping the relationship between the input and the output using the back-propagation algorithm has been widely demonstrated [57]. In this paper, four different neural networks have been used for prediction of solar irradiance, air temperature, electricity price and carbon intensity.

The first two neural networks are used for prediction of solar irradiance and air temperature, and are obtained from [30]. They work with 15 minutes sampling time, so that the available profiles have been interpolated to obtain a 15-minutes time step, processed through the neural network, and resampled to get predictions with 1-hour time step. The ANN architecture consists of one input layer with 12 neurons corresponding to the previous 12 input values from time k back to time k-11, one or more hidden layers within a number of neurons estimated during the training process, and one output layer containing 12 output values corresponding to time steps from $k+1$ up to k+12, as depicted in Figure 3. The dataset used for the training of the network consists of the 35136 samples. This dataset has been restructured as a matrix of NxM dimension where N=12 rows and M=35124 columns. The FFNN prediction model can be simply formulated as:

$$Y^N\left(k+1\right) = FFNN\left(Y^N\left(k\right)\right) \qquad (22)$$

where Y^N (k) is the columns k, Y^N(k+1) corresponds to the next columns (k+1) and $N = 1, 2, \ldots, 12$. The dataset has been divided into two sets: the 80% of the samples has been used for the training, while the remaining 20% has been used for testing the model. With reference to Figure 4, during the first iteration the input and the output of the FFNN correspond the first and the second columns, respectively. During the second iteration, the input and the output the FFNN correspond to the second and the third columns, respectively. The method is applied in the same way until the mean square error is less than 10%. The FFNN is then able to predict the next 12 values of solar irradiance and air temperature based on the actual values of the previous 12. The training process has been tuned using the Levenberg-Marquardt algorithm [58] which is available in MATLAB using the *trainlm* network training function [59]. After a number of experiments, the best configuration has been obtained with the structure 12x15x12 (12 neurons in the input layer, 15 in the hidden layer and 12 in the output layer). Considering the final resample of prediction data, the considered ANN provides a forecast of the next three hours, based on the measures over the last three hours.

A similar approach has been used to design the other neural networks used in this paper, which are aimed at forecasting carbon intensity and price. For carbon intensity predictions, the ANN architecture consists of one input layer with 24 neurons corresponding to the previous 24 input values from time k back to time k - 23, one or more hidden layers within a number of neurons estimated during the training process, and one output layer containing 3 output values corresponding to time steps from $k+1$ up to k+3, as depicted in Figure 3. The dataset used for the training of the network consists of the 52591 samples. This dataset has been restructured as a matrix of NxM dimension where N=24 rows and M=52527 columns. The FFNN prediction

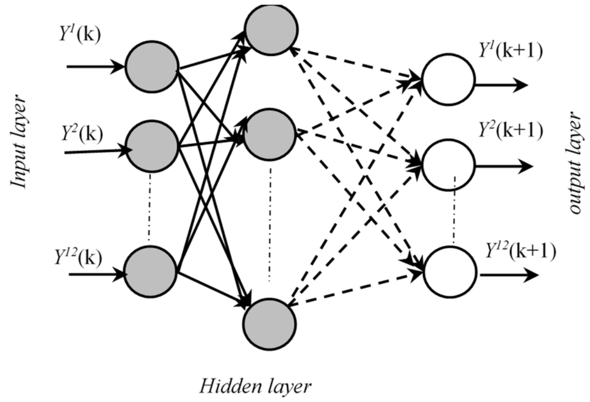

Figure 3. Feed forward neural network configuration

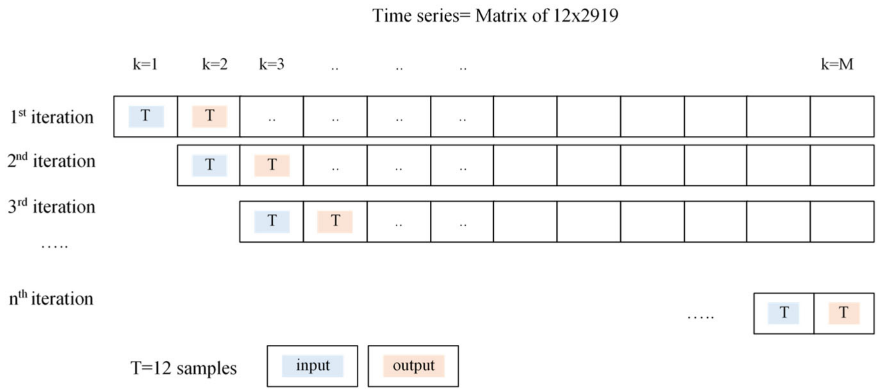

Figure 4. Multistep ahead forecasting scheme

model can be simply formulated as (22), with $N = 1, 2, \dots, 24$. The dataset has been divided into two sets: the 85% of the samples has been used for the training, while the remaining 15% has been used for testing the model. The method is applied in the same way until the mean square error is less than 10%. The FFNN is then able to predict the next 3 values of carbon intensity equivalent emissions based on the actual values of the previous 24. The training process has been tuned using the Levenberg-Marquardt algorithm. After a number of experiments, the best configuration has been obtained with the structure 24x12x3 (24 neurons in the input layer, 12 in the hidden layer and 3 in the output layer). For price predictions, the same procedure used for carbon intensity predictions has been used. In particular, The ANN architecture consists of one input layer with 9 neurons corresponding to the previous 9 input values from time k back to time k - 8, one or more hidden layers within a number of neurons estimated during the training process, and one output layer containing 3 output values corresponding to time steps from $k+1$ up to k+3, as depicted in Figure 3. The dataset used for the training of the network consists of the 54295 samples. This dataset has been restructured as a matrix of NxM dimension where N=24 rows and M=54244 columns. The training process has been tuned using the Levenberg-Marquardt algorithm. The resulting FFNN is then able to predict the next 3 values of electricity price based on the actual values of the previous 24. After a number of experiments, the best configuration has been obtained with the structure 9x12x3 (9 neurons in the input layer, 12 in the hidden layer and 3 in the output layer).

3.4.3. Integration of Real-time Measures and ANN predictions with statistical data.

The forecasts provided by the ANN-based predictor are than integrated in the overall forecasts: at each time step, the previous 3 measured values of solar irradiance and air temperature are provided as input to the ANN-based predictor, which provides a forecast of the 3 subsequent values of the same quantities. These 3 values substitute the corresponding 3 values of the statistical profiles described in Section 3.4.1, so that, at each time step, the first 3 steps of the forecasts are those provided by the ANN, while the following steps are purely statistical forecasts. The same is done for price and carbon intensity ANN, which, even though requiring a different number of inputs, still provide as output a 3-hour prediction.

This solution produces adaptive forecasts of the considered quantities, which are updated based on real-time measures at each time step. A similar approach based on averaging of real-time measures and statistical forecasts was proposed in [60] for this same task. However, the addition of the ANN-based predictor proposed in this paper significantly increases the accuracy of short-term prediction, which has the most effect on MPC control action, with minimal computational burden increase. The statistical forecast proposed [60] is used, in this paper, as a way to ensure a smooth transition between ANN predictions and statistical data.

Overall, at each time step k, the real time measure is acquired, the step [k+1; k+3] are the forecasts provided by the ANN, and the subsequent three steps [k+4; k+6] are obtained by means of the statistical forecast proposed in [60] to ensure a smooth connection between ANN prediction and statistical data.

Considering load forecasts, the high volatility of the considered profiles made impossible to use a simple FFNN to generate useful prediction. Indeed, the complexity of the load profile generator [46] used to generate them suggest that a very complex network must be used to obtain reasonable predictions, which is in contrast with the simplicity target of this paper. Consequently, the statistical forecast proposed in [60] has been used to connect real-time measures and statistical predictions, with no further forecast techniques applied.

4. System Simulation and Numerical Results

In this Section, the numerical simulations performed to assess the effectiveness of the proposed MPC controller are reported. All simulations have been realized as MATLAB code and cover one year of operation. The considered simulations scenarios are described in Section 4.1, necessary numerical data are reported in Section 4.2, simulation results are presented in Section 4.3, while an economic analysis of the presented results is reported in Section 4.4. Global results are discussed in Section 4.5.

4.1. Definition of Simulation Scenarios.

In order to assess the proposed control effectiveness, a comprehensive set of simulations have been performed. The considered simulation scenarios are reported in the following.

4.1.1. Simulation Scenario 1: First Benchmark Simulation.

In this scenario, no optimization is performed, and no measures are shared between connection points. The battery is controlled considering only the measures available at the common utility meter (CM) in Figure 1. The power drained from the battery, at each time step k, is calculated as

$$P_{batt}(k) = \begin{cases} \operatorname{sgn}\left(P_{PV} - E(13,k)\right)\left(E(13,k) - P_{PV}(k)\right) & if\, 1 - DOD \le SOC(k) - P_{batt}(k)\dfrac{\Delta t}{C_{batt}} \le 1 \\ 0 & otherwise \end{cases} \tag{23}$$

Simulation Scenario 1 basically covers what would be done at the moment in terms of energy management, and will be considered a first reference for the evaluation of optimized simulations. In this case, the battery is charged and discharged in order to cover, if possible, the load at the common utility meter (CM), maximizing its self-consumption. The excess of generation is stored in the ESS for later use for common services if possible, otherwise it is injected into the distribution grid. In this latter case, part of the injected energy will be considered shared energy, depending on the absorptions at the other 12 connection points.

4.1.2. Simulation Scenario 2: Second Benchmark Simulation.

In this scenario, no optimization is performed, but measures from connection points 1-12 are shared among JARSCs. The battery is controlled considering the measures available at the 13 connection points in Figure 1. The power drained from the battery, at each time step k, is calculated as

$$P_{batt}(k) = \begin{cases} \operatorname{sgn}\left(P_{PV}(k) - \sum_{i=1}^{13} E(i,k)\right)\left(\sum_{i=1}^{13} E(i,k) - P_{PV}(k)\right) & if\, 1 - DOD \le SOC(k) - P_{batt}(k)\dfrac{\Delta t}{C_{batt}} \le 1 \\ 0 & otherwise \end{cases} \tag{24}$$

Scenario 2 represents a significant improvement over Scenario 1 and is specifically tailored for JARSCs. Consequently, it will be considered a second reference for the evaluation of optimized simulations. In this case, the battery is charged and discharged in order to cover, if possible, the global load at the 13 connection points, maximizing self-consumption and energy shared among JARSCs. The excess of generation is stored in the ESS for later use at among JARSCs if possible, otherwise it is injected into the distribution grid and sold.

4.1.3. Simulation Scenario 3: First Optimization Solution.

In this scenario, the considered problem is addressed by means of the MPC controller discussed in Section 3.2, including constraints (13) - (16), but not constraint (17), and cost function weight $\gamma = 0$. Forecasts obtained according to Section 3.4 are used. Cost functions weights α, β are varied from 0 to 1 by 0.1 steps, with $\alpha + \beta = 1$, resulting in a set of eleven simulations highlighting the effect of different (arbitrary) priorities in the optimization problem.

4.1.4. Simulation Scenario 4: Second Optimization Solution.

In this scenario, the considered problem is addressed by means of the MPC controller discussed in Section 3.2, including constraints (13) - (17), and cost function weight $\gamma = 1$. Forecasts obtained according to Section 3.4 are used. Cost functions weights α, β are varied from 0 to 1 by 0.1 steps, with $\alpha + \beta = 1$. As mentioned, the additional constraint (17) does not allow the MPC controller to buy energy from the grid to charge the battery, which is often contrary to the spirit of reducing CO2 emissions, at least as long as the energy mix includes fossil fuels. The additional cost term included in the optimization problem by setting $\gamma = 1$ adds an additional cost to energy sold while the battery is not fully charged, which represents a form of caution against forecast errors. In fact, the MPC controller may decide not to charge the battery and to sell energy during the morning, planning to charge the battery at noon, when the price is usually lower. However, an error in forecasts (e.g. unforeseen shading) can make impossible to charge the battery when planned, causing a lack of energy during the evening and night, which will force the MPC controller to buy energy from the grid increasing costs and CO2 equivalent emissions.

4.1.5. Simulation Scenario 5: Third Optimization Solution.

In this scenario, the considered problem is addressed by means of the MPC controller discussed in Section 3.2, including constraints (13) - (16), but not constraint (17), and cost function weight $\gamma = 0$. Ideal forecasts (e.g. perfect forecast of each quantity the forecast of which is used in the optimization problem) are used. Cost functions weights α, β are varied from 0 to 1 by 0.1 steps, with $\alpha + \beta = 1$. This solution is obviously not feasible in real applications, in that any forecast method will include a certain level of uncertainty. However, it may be useful to consider this scenario too, as it represents the best possible solution of the considered optimization problem, which could be reached in principle with very accurate predictors.

4.2. Numerical Data.

In this Section, the numerical data necessary for simulation are reported. In addition to the data referenced in Section 2.2, to determine electricity price it is necessary to calculate fixed costs, energy buying price and energy selling price. Fixed costs are here calculated according to the Italian standard and are available from [61]. They consist of a fixed component and of a component proportional to the contractual power. The numerical values of these fixed cost, for each connection point, are reported in Table 4. Energy selling price is assumed equal to the PO referenced in Section 2.2. Energy buying price is determined considering that, during 2016, the energy component of buying price was, on average, equal to selling price increased by 89 %. In addition to energy component, there is another component to be considered, including various fees and customs, on average equal to 0.0586 €/kWh. Lastly, VAT is equal to 10 % for the 12 residential connection points, while it is equal to 22 % for the last, non-residential connection point.

4.3. Simulation Results.

Numerical results from the simulation scenarios detailed in Section 4.1 are reported in this Section. As mentioned, the performance indexes used for the evaluation of the presented results are the total electricity cost [€] charged to the JARSCs over one year and the total CO2 equivalent emissions [kg] generated by the electrical system to provide the JARSCs the total amount of energy bought from the grid over one year. Additional quantities of interest are: total energy [kWh] drained from the ESS over one year, total shared energy [kWh] over one year and total self-consumed energy [kWh] over one year. For ease of comparison among different scenarios, the results in terms of electricity cost [€], total CO2 equivalent emissions [kg], total energy [kWh] drained from the ESS, total shared energy [kWh], total self-consumed energy [kWh] are reported, respectively, in Table 5, Table 6, Table 7, Table 8, and Table 9. Additionally, the results of the optimization problem (electricity cost [€], total CO2 equivalent emissions [kg]) are graphically presented in Figure 5. For reference, the electricity cost and CO2 equivalent emissions have also been calculated based only of load profiles, which corresponds to what JARSCs would have been charged in absence of PV and ESS. The total cost is, in this case, equal to 9189 €, while the total equivalent CO2 emissions are equal to 17175 kg.

4.3.1. Simulation Scenario 1: First Benchamrk Simulation.

As mentioned, this scenario represents the basic benchmark for performance evaluation. The total cost in charge to the JARSCs is equal to 5972 €, while the total CO2 equivalent emissions are equal to 11204 kg. The total energy drained from the ESS over one year is equal to 6632 kWh, total shared energy over one year is equal to 4648 kWh and total self-consumed energy over one year is

TABLE 4 – JARSCS FIXED ELECTRICITY COSTS

Connection point	Cost [€/year]	Connection point	Cost [€/year]
UM 1	143.81	UM 8	143.81
UM 2	143.81	UM 9	133.19
UM 3	154.43	UM 10	154.43
UM 4	175.67	UM 11	133.19
UM 5	175.67	UM 12	133.19
UM 6	143.81	CM	600.47
UM 7	143.81		

TABLE 5 – JARSCS TOTAL ELECTRICITY COST [€] OVER ONE YEAR

Scen. 1	Scen. 2	Scen. 3	Scen. 4	Scen. 5	α
		5810	5398	5495	0
		5536	5298	5166	0.1
		5469	5264	5069	0.2
		5438	5247	5023	0.3
		5418	5238	5000	0.4
5972	5371	5408	5233	4991	0.5
		5401	5230	4987	0.6
		5399	5228	4985	0.7
		5397	5228	4984	0.8
		5394	5227	4984	0.9
		5393	5227	4984	1

TABLE 6 – JARSCS TOTAL CO2 EMISSIONS [KG] OVER ONE YEAR

Scen. 1	Scen. 2	Scen. 3	Scen. 4	Scen. 5	α
		9261	8541	7959	0
		9328	8467	8085	0.1
		9334	8452	8248	0.2
		9401	8438	8400	0.3
		9454	8442	8521	0.4
11204	8854	9497	8445	8590	0.5
		9535	8453	8633	0.6
		9574	8461	8662	0.7
		9590	8469	8686	0.8
		9603	8467	8711	0.9
		9618	8473	8734	1

TABLE 7 – JARSCS TOTAL ENERGY [KWH] DRAINED FROM THE ESS OVER ONE YEAR

Scen. 1	Scen. 2	Scen. 3	Scen. 4	Scen. 5	α
		13312	10627	16204	0
		11173	10543	14263	0.1
		11054	10669	14369	0.2
		11331	10778	15185	0.3
		11637	10834	15860	0.4
6632	9317	11891	10877	16241	0.5
		12144	10907	16452	0.6
		12333	10912	16586	0.7
		12429	10934	16722	0.8
		12526	10959	16831	0.9
		12619	10973	16900	1

TABLE 8 – JARSCS TOTAL SHARED ENERGY [KWH] OVER ONE YEAR

Scen. 1	Scen. 2	Scen. 3	Scen. 4	Scen. 5	α
		15949	14651	18120	0
		13206	13906	15237	0.1
		12963	13738	14600	0.2
		13254	13841	14934	0.3
		13600	13933	15461	0.4
4648	14749	13881	13986	15834	0.5
		14123	14031	16072	0.6
		14306	14068	16229	0.7
		14387	14077	16332	0.8
		14482	14077	16436	0.9
		14536	14104	16504	1

TABLE 9 – JARSCS TOTAL SELF-CONSUMED ENERGY [KWH] OVER ONE YEAR

Scen. 1	Scen. 2	Scen. 3	Scen. 4	Scen. 5	α
		7094	6550	8869	0
		7442	7594	9193	0.1
		7764	7894	9952	0.2
		7800	7888	10458	0.3
		7855	7842	10622	0.4
10322	6277	7872	7822	10650	0.5
		7899	7789	10651	0.6
		7934	7761	10633	0.7
		7964	7748	10666	0.8
		7976	7759	10679	0.9
		8009	7730	10687	1

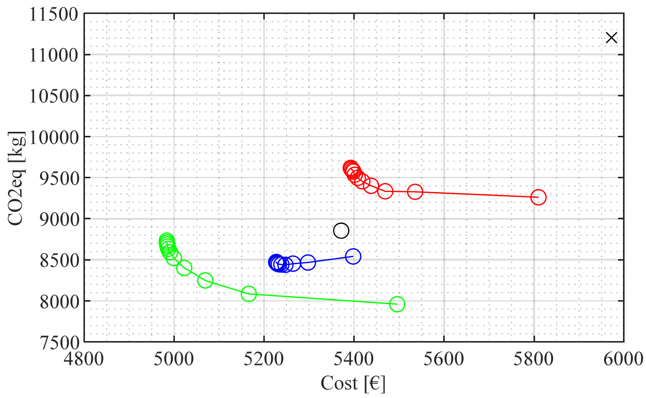

Figure 5. Graphical representation of simulation results: scenario 1 (black cross), scenario 2 (black circle), scenario 3 (red), scenario 4 (blue), scenario 5 (green)

equal to 10322 kWh. The results of the optimization problem (electricity cost [€], total CO2 equivalent emissions [kg]) are identified by a black cross in the solution plane (€ - CO2) graphically presented in Figure 5.

4.3.2. Simulation Scenario 2: Second Benchamrk Simulation.

This second scenario represents a significant improvement over Scenario 1, in that the measures from connection points 1 – 12 are collected and used to consider shared energy, in addition to self-consumption, in battery management. The total cost in charge to the JARSCs is equal to 5371 €, while the total CO2 equivalent emissions are equal to 8854 kg. This corresponds to a 10.1 % cost reduction and 21.0 % CO2 emissions reduction. The total energy drained from the ESS over one year is equal to 9317 kWh, total shared energy over one year is equal to 14749 kWh and total self-consumed energy over one year is equal to 6277 kWh. With respect to Scenario 1, the energy drained from the ESS is increased by 40.5 %, self-consumed energy is reduced by 39.2 % and shared energy is increased by 217.4 %. Even though self-consumed energy is the most effective remuneration mechanism for small PV generators, which would suggest that Scenario 2 would not provide any advantage over Scenario 1, the change of the control law from (23) (Scenario 1) to (24) (Scenario 2) generates a huge increase in shared energy which, unitedly with the incentive on shared energy selling price, produces a significant improvement in cost and CO2 emissions over Scenario 1. This can be clearly seen in the graphical representation reported in Figure 5, where the results of the optimization problem in Scenario 2 are identified by a black circle.

4.3.3. Simulation Scenario 3: First Optimization Solution.

This scenario represents the first optimized solution proposed in this paper. The results in terms of electricity cost [€], total CO2 equivalent emissions [kg], total energy [kWh] drained from the ESS, total shared energy [kWh], total self-consumed energy [kWh] are reported, respectively, in Table 5, Table 6, Table 7, Table 8, and Table 9, for the complete considered range of cost function weights α, β. Simulations were performed using a common desktop PC with an Intel Core i5-7500 CPU and 16 GB RAM. The average computational time required for each iteration of the MPC control is equal to 205 ms. Considering that no particular attention has been dedicated to computational efficiency and that the considered sample time is equal to 1 hour, this is more than satisfactory and supports the applicability of the proposed control to real-time applications, with no need for excessive computational requirements.

The minimum total cost in charge to the JARSCs is equal to 5393 €, while the minimum total CO2 equivalent emissions are equal to 9261 kg. The complete set of results of the optimization problem (electricity cost [€], total CO2 equivalent emissions [kg]) are identified by red circles in the solution plane (€ - CO2) graphically presented in Figure 5, which exhibits the quite regular behaviour expected from the Pareto frontier of optimization problems. However, Figure 5 also clearly shows that Scenario 3 introduces significant advantage over Scenario 1, but it does not provide better performance than Scenario 2. Further investigation of this disappointing result revealed that the main problem with the optimization problem addressed in Scenario 3 is the relative slow update of the forecasts used. This is caused partially by the inevitable delays in prediction responses, partially to the 1-hour sampling time. This creates two main issues:

- the MPC may decide to buy from the grid to charge the battery in prevision of future use, depending on generation, load, carbon intensity and price forecasts. However, this operation is dangerous, in that inevitable errors in previsions may compromise the advantages that the MPC controller planned to obtain. Additionally, buying energy from the grid to charge the ESS may be considered not desirable in terms of CO2 emissions in general.
- the MPC controller may decide not to charge the battery and to sell energy during the morning, and to charge the battery at noon, when the price is usually lower. However, an error in forecasts (e.g. unforeseen shading) can make impossible to charge the battery when planned, causing a lack of energy during the evening and night, which will force the MPC controller to buy energy from the grid increasing costs and CO2 equivalent emissions.

On the basis of these considerations, Scenario 4 was developed by adding the additional constraint (17), which does not allow the MPC controller to buy energy from the grid to charge the battery, and setting $\gamma = 1$. The additional cost term included therefore in the optimization problem adds an additional cost to energy sold while the battery is not fully charged, which represents a form of caution against forecast errors.

4.3.4. Simulation Scenario 4: Second Optimization Solution.

This Scenario represents the second optimized solution proposed in this paper, in which, in order to avoid the issue emerged in Section 4.3.3 for Scenario 3, the cost function weight γ is set $\gamma = 1$ and the additional constraint (17) is included in the optimization problem. The results in terms of electricity cost [€], total CO2 equivalent emissions [kg], total energy [kWh] drained from the ESS, total shared energy [kWh], total self-consumed energy [kWh] are reported, respectively, in Table 5, Table 6, Table 7, Table 8, and Table 9, for the complete considered range of cost functions weights α, β. Simulations were performed using a common desktop PC with an Intel Core i5-7500 CPU and 16 GB RAM. The average computational time required for each iteration of the MPC control is equal to 285 ms, which is more than satisfactory and supports the applicability of the proposed control to real-time applications.

The minimum total cost in charge to the JARSCs is equal to 5227 €, while the minimum total CO2 equivalent emissions are equal to 8438 kg. This corresponds to a cost reduction up to 12.5 % and a CO2 emissions reduction up to 24.7 % with respect to Scenario 1, and to a cost reduction up to 2.7 % and a CO2 emissions reduction up to 4.7 % with respect to Scenario 2. The maximum total energy drained from the ESS over one year is equal to 10973 kWh, maximum total shared energy over one year is equal to 14651 kWh and maximum total self-consumed energy over one year is equal to 7894 kWh. With respect to Scenario 1, the energy drained from the ESS is increased up to 65.5 %, self-consumed energy is increased up to 3.5 % and shared energy is increased up to 215.2 %. With respect to Scenario 2, the energy drained from the ESS is increased up to 17.8 %, self-consumed energy is increased up to 70.3 % and shared energy is decreased at least of 0.6 %. These results highlight that the optimized solution considered in Scenario 4 produces a total shared energy close to the non-optimized solution considered in Scenario 2. However, the optimized solution manages to significantly increase self-consumed energy, which produces benefits in cost and CO2 emission reduction, at expense of more demanding battery use. The complete set of results of the optimization problem (electricity cost [€], total CO2 equivalent emissions [kg]) are identified by blue circles in the solution plane (€ - CO2) graphically presented in Figure 5, which clearly shows the advantage gained by means of the proposed MPC controller with respect to non-optimized solution. In the meantime, Figure 5 also shows that the Pareto frontier associated with this optimization problem is not similar to the usually expected hyperbola. This is due to the fact that the additional cost term introduced in Scenario 4 affects the solution of the optimization problem, impeding the MPC to sell energy while the battery is not charged, while the additional constraint (17) does not allow the MPC to buy energy to charge the battery. However, Figure 5 shows only two cost terms, which makes impossible to graphically appreciate the effect of three cost terms (a 3-D surface with parametrization of α, β, γ would be necessary). Still, Figure 5 highlights that setting $\alpha < 0.3$ is useless in this scenario, in that the additional cost terms and constraint do not allow for a reduction in CO2 emissions, such that setting $\alpha < 0.3$ implies an increase in cost, but not a reduction of CO2 emissions. Still, it is clear that the additional cost term and constraints allow the MPC to improve over non-optimized solutions and take advantage of available forecasts, the errors included in which were critical for the MPC formulation discussed in Section 4.3.3.

4.3.5. Simulation Scenario 5: Third Optimization Solution.

This scenario represents the third and last optimized solution proposed in this paper, which is intended to disclose the full potential of the considered MPC control. As mentioned, the additional cost and constraints introduced in Scenario 4 are ditched, and the forecast obtained by the techniques discussed in Section 3.4 are substituted with ideal predictions, identical to measured data. While the applicability of this scenario is questionable, it is useful to consider it in this Section as it allows to identify the theoretical optimal solution which would be obtained with perfect predictions, providing a measure of the possible improvement theoretically available over Scenario 4. The results in terms of electricity cost [€], total CO2 equivalent emissions [kg], total energy [kWh] drained from the ESS, total shared energy [kWh], total self-consumed energy [kWh] are reported, respectively, in Table 5, Table 6, Table 7, Table 8, and Table 9, for the complete considered range of cost functions weights α, β. Simulations were performed using a common desktop PC with an Intel Core i5-7500 CPU and 16 GB RAM. The average computational time required for each iteration of the MPC control is equal to 205 ms, which is more than satisfactory and supports the applicability of the proposed control to real-time applications.

The minimum total cost in charge to the JARSCs is equal to 4984 €, while the minimum total CO2 equivalent emissions are equal to 7959 kg. This corresponds to a cost reduction up to 16.5 % and a CO2 emissions reduction up to 29.0 % with respect to Scenario 1, and to a cost reduction up to 7.2 % and a CO2 emissions reduction up to 10.1 % with respect to Scenario 2, and to a cost reduction up to 4.7 % and a CO2 emissions reduction up to 5.7 % with respect to Scenario 4. The maximum total energy drained from the ESS over one year is equal to 16900 kWh, maximum total shared energy over one year is equal to 18120 kWh and maximum total self-consumed energy over one year is equal to 10687 kWh. With respect to Scenario 1, the energy drained from the ESS is increased up to 154.8 %, self-consumed energy is increased up to 3.5 % and shared energy is increased up to 289.8 %. With respect to Scenario 2, the energy drained from the ESS is increased up to 81.4 %, self-consumed energy is increased up to 70.3 % and shared energy is increased up to 22.9 %. With respect to Scenario 4, the energy drained from the ESS is increased up to 54.0 %, self-consumed energy is increased up to 35.5 % and shared energy is increased up to 23.7 %.

4.4. Economic Analysis.

In this Section, a basic analysis of the common economic indicators used for PV/ESS analysis is reported. Quantities considered are: Levelized Cost of Energy (LCOE) [€cent/kWh], Levelized Cost of Storage (LCOS) [€cent/kWh], payback time [years], Net Present Value (NPV) [k€], and annual revenue per user [€]. Methodologies for calculation of the aforementioned indicators can be found in [62], [63]. The main data used for calculation of economic indicators are reported in Table 10. The numerical values of the considered economic indicators, for each considered Scenario, are reported in Table 11. A graphical representation of the NPV behaviour over the expected life of the PV/ESS system for Scenarios 1, 2, and 4 is presented in Figure 6, where, for Scenario 4, the less favourable result is reported in orange, while the most favourable result is reported in blue. Since Scenario 3 proved to be of scarce interest and Scenario 5 is intended just as a limit optimal solution, only Scenarios 1, 2, and 4 are discussed.

The LCOE, depending only on PV cost and PV production, is common to all scenarios and equal to 8.87 €cent/kWh. The LCOS is equal to 18.32 €cent/kWh in Scenario 1, which is reduced to 13.04 €cent/kWh in Scenario 2 and up to 11.07 €cent/kWh in Scenario 4, due to the increased use of ESS for energy sharing among JARSCs. The payback time is equal to 15 years in Scenario 1, while it is equal to 13 years in Scenarios 2 and can be reduced to up to 12 years in Scenario 4. NPV is equal to 20.74 k€ in Scenario 1, 35.26 k€ in Scenario 2 and increases up to 38.74 k€ in Scenario 4. Annual revenues per user are equal to 57.62 € in Scenario 1, 97.94 € in Scenario 2 and increase up to 107.60 € in Scenario 4. Overall, the economic indicators are not particularly favourable, in that, while it is clear that the installation of the combined PV/ESS system does produce revenues over the expected life of the system, the entity of these revenues is not very significant and payback time are quite long. On the other side, it must be

TABLE 10 – JARSCS ECONOMIC PARAMETERS

Parameter	Value	Parameter	Value
System expected life	20 years	Yield of the plant over the first year of operation	1100 kWh/kWp
Return of equity	0.1 %	Fixed operation and maintenance costs	1 %
Return of debt	4 %	Battery cost	900 €/kWh
Equity percentage	50 %	Tax deduction	50% in 10 years
Debt percentage	50 %	Inflation rate	2 %
PV cost	1540 €/kWp	Energy inflation rate	2 %
PV degradation rate	0.25 %	Interest rate	2 %

Table 11 – Economic Indicators

	Scenario 1	Scenario 2	Scenario 4
LCOE [€cent/kWh]	8.87	8.87	8.87
LCOS [€cent/kWh]	18.32	13.04	11.07 - 11.52
Payback Time [years]	15	13	12 - 13
NPV [k€]	20.74	35.26	34.61 - 38.74
Annual Revenue per User [€]	57.62	97.94	96.13 - 107.60

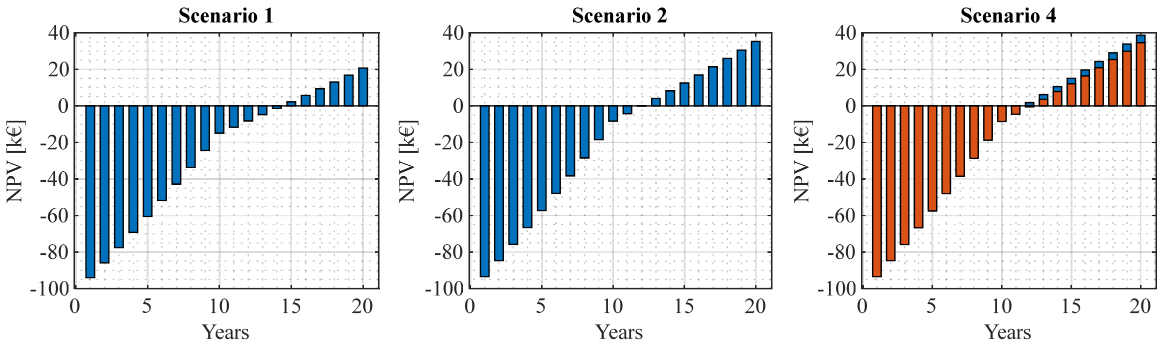

Figure 6. Graphical representation of NPV behaviour over the expected life of the PV/ESS system for Scenarios 1, 2, and 4.

considered that the equivalent CO2 emission, not considered in economic analysis, are reduced from 17175 kg up to 7959 kg, which corresponds to a reduction up to 53.7 %. Considering the target of decarbonization driving the European Directives of reference for RECs and JARSCs, this may be considered quite a significant result. Additionally, it is not hard to foresee that equivalent CO2 emissions, which at the moment represent an additional cost only for large industrial loads, may in the not so far future be an additional cost also of residential users. In this case, the significant reduction in CO2 emissions would produce significant economic savings.

4.5. Discussion of Simulation Result.

From a technical perspective, the results discussed in Section 4.3 show that the proposed MPC controller introduces significant advantages with respect to not optimized solutions, as long as predictions are sufficiently accurate or specific measures to reduce sensitivity to forecasts errors are included in the optimization problem formulation. In these regards, the following issues could be addressed to further improve control performances:

- smaller sampling time: in principle, a smaller sampling time would reduce the sensitivity to forecast errors, in that it allows the MPC controller to re-evaluate its control action more frequently. The MPC controller discussed in this paper, due to the 1-hour sampling time, cannot update its control action for one hour after each solution of the optimization problem, which may be a problem in presence of inaccurate forecasts. On the other side, a smaller time step would increase computational burden. However, the results shown in Section 4.3 suggest that computational time would not be a significant issue. A smaller sampling time would also be beneficial for PV production ANN-based forecaster, in that it would update its prediction more frequently considering real-time measures;
- improved predictors: more efficient predictors would take the solution obtained in Scenario 4 closer to the theoretical optimum discussed in Scenario 5. On the other side, this possible solution is to be cautiously evaluated, since the additional complexity of improved predictors may not be compatible with real-time applications;
- load side demand control: the introduction of demand control policies may produce significant benefits in optimized scenarios, in that load volatility has proven difficult to be predicted. Load side demand control policies would help in that they would make load more regular and predictable, allowing more efficient optimization, and may also allow to partially reshape the load profiles with respect to generation, price and carbon intensity profiles, allowing a further degree of freedom in the optimization problem.

From an economic perspective, the results discussed in Section 4.4 highlights that the considered solution does produce revenues over its expected life, but the entity of these revenues is not enough to be an attractive investment form. These results also allow drawing some considerations regarding the incentive plan for JARSCs currently available in Italy. On one side, it is clear that the incentive plan does create an economic advantage for prosumers sharing energy among a group of JARSCs or REC, which is beneficial for the environment in terms of CO2 emission reduction, and beneficial for the distribution system, which is less likely to suffer from excessive generation. This suggest that, if economic convenience is the main target, a smaller PV/ESS would be better suited for the task, having a shorter payback time due to a higher self-consumption, but generating less savings in terms of electricity bill and smaller reductions in the CO2 emissions. On the other side, the entity of the incentive is not sufficient to make the installation of a PV/ESS an attractive investment for the energy sharing mechanism. Two possible ways to increase profitability are foreseen:

- remuneration of CO2 emissions reduction: considering that decarbonization is the driving reason for recent changes in energy market, extending a form of remuneration of CO2 emission reduction to residential users is reasonable. Considering that the reduction in CO2 emissions are very significant when, as in this paper, the PV/ESS system is designed to cover most of the JARSCs energy needs, an economic recognition of this result would significantly increase profitability of larger PV/ESS systems over smaller ones, which would perfectly fit the decarbonization task;
- power sharing solutions: physical power sharing [13], not using the DSO system as a mean for virtual energy exchange, would not benefit from incentive on shared energy. However, the average energy selling price resulting from the present study, including incentives, is roughly equal to 16 €cent/kWh, while the energy buying price is, on average, roughly equal to 24 €cent/kWh. From these data, the increased self-consumption obtained from power sharing would be 50 % more convenient that sharing energy through the DSO infrastructure. On the other side, the power sharing requires additional converters, cables and switchboards, the cost of which is to be included in economic evaluation. However, this study seems to suggest that power sharing, even if not yet covered by standards, may be a more profitable solution than virtual energy exchange through the DSO grid.

5. Conclusions

In this paper, an MPC-based control algorithm coupled with an ANN-based predictor for optimal management of JARSCs is presented. The proposed algorithm evaluates the control action over a one-day prediction horizon, considering available forecasts of PV production, electricity price, carbon intensity and load, and minimizes a cost function including electricity cost and equivalent CO2 emissions. Five simulation scenarios are presented and discussed, highlighting the effectiveness of the proposed control design, which produces a cost reduction up to 12.5 % and a CO2 emissions reduction up to 24.7 %. An essential economic evaluation of the considered system shows that the revenues are not large and payback time are quite long, but reduction in CO2 emissions up to 53.7 % are obtained by means of the considered PV/ESS system. Lastly, a brief discussion identified the main technical and economic aspects worth of further study in order to improve the considered system performance.

References

[1] Directive (EU) 2018/2001 of the European Parliament and of the Council of 11 December 2018 on the promotion of the use of energy from renewable sources, http://data.europa.eu/eli/dir/2018/2001/2018-12-21.

[2] Directive (EU) 2019/944 of the European Parliament and of the Council of 5 June 2019 on common rules for the internal market for electricity and amending Directive 2012/27/EU, http://data.europa.eu/eli/dir/2019/944/oj.

[3] Directive 2003/87/EC of the European Parliament and of the Council of 13 October 2003 establishing a system for greenhouse gas emission allowance trading within the Union and amending Council Directive 96/61/EC, http://data.europa.eu/eli/dir/2003/87/2021-01-01.

[4] S. Cejka, D. Frieden, e D. Kitzmüller, «Implementation of self-consumption and energy communities in Austria's and EU member states' national law: A perspective on system integration and grid tariffs», in *CIRED 2021 - The 26th International Conference and Exhibition on Electricity Distribution*, set. 2021, vol. 2021, pagg. 3254–3258. doi: 10.1049/icp.2021.1526.

[5] D. Frieden, A. Tuerk, J. Roberts, S. D'Herbemont, A. F. Gubina, e B. Komel, «Overview of emerging regulatory frameworks on collective self-consumption and energy communities in Europe», in *2019 16th International Conference on the European Energy Market (EEM)*, set. 2019, pagg. 1–6. doi: 10.1109/EEM.2019.8916222.

[6] M. L. Di Silvestre, M. G. Ippolito, E. R. Sanseverino, G. Sciumè, e A. Vasile, «Energy self-consumers and renewable energy communities in Italy: New actors of the electric power systems», *Renewable and Sustainable Energy Reviews*, vol. 151, pag. 111565, nov. 2021, doi: 10.1016/j.rser.2021.111565.

[7] European Commission, Joint Research Centre, Uihlein, A., Caramizaru, A. (2020). Energy communities : an overview of energy and social innovation, Publications Office. https://data.europa.eu/doi/10.2760/180576.

[8] Catalina Alexandra Sima, Claudia Laurenta Popescu, Mihai Octavian Popescu, Mariacristina Roscia, George Seritan, Cornel Panait, "Techno-economic assessment of university energy communities with on/off microgrid," Renewable Energy, Volume 193, 2022, Pages 538-553.

[9] L. Herenčić, M. Kirac, H. Keko, I. Kuzle, e I. Rajšl, «Automated energy sharing in MV and LV distribution grids within an energy community: A case for Croatian city of Križevci with a hybrid renewable system», *Renewable Energy*, vol. 191, pagg. 176–194, mag. 2022, doi: 10.1016/j.renene.2022.04.044.

[10] G. Barone *et al.*, «How Smart Metering and Smart Charging may Help a Local Energy Community in Collective Self-Consumption in Presence of Electric Vehicles», *Energies*, vol. 13, n. 16, Art. n. 16, gen. 2020, doi: 10.3390/en13164163.

[11] Z. de Grève *et al.*, «Machine learning techniques for improving self-consumption in renewable energy communities», *Energies*, vol. 13, n. 18, 2020, doi: 10.3390/en13184892.

[12] G. P. Luz, M. C. Brito, J. M. C. Sousa, e S. M. Vieira, «Coordinating shiftable loads for collective photovoltaic self-consumption: A multi-agent approach», *Energy*, vol. 229, pag. 120573, ago. 2021, doi: 10.1016/j.energy.2021.120573.

[13] G. Di Lorenzo, S. Rotondo, R. Araneo, G. Petrone, e L. Martirano, «Innovative power-sharing model for buildings and energy communities», *Renewable Energy*, vol. 172, pagg. 1087–1102, lug. 2021, doi: 10.1016/j.renene.2021.03.063.

[14] M. Zatti, M. Moncecchi, M. Gabba, A. Chiesa, F. Bovera, e M. Merlo, «Energy Communities Design Optimization in the Italian Framework», *Applied Sciences*, vol. 11, n. 11, Art. n. 11, gen. 2021, doi: 10.3390/app11115218.

[15] E. S. Pinto, L. M. Serra, e A. Lázaro, «Optimization of the design of polygeneration systems for the residential sector under different self-consumption regulations», *International Journal of Energy Research*, vol. 44, n. 14, pagg. 11248–11273, 2020, doi: 10.1002/er.5738.

[16] I. D'Adamo, «The profitability of residential photovoltaic systems. A new scheme of subsidies based on the price of CO2 in a developed PV market», *Social Sciences*, vol. 7, n. 9, pag. 148, 2018.

[17] A. Sierra Rodriguez, T. de Santana, I. MacGill, N. j. Ekins-Daukes, e A. Reinders, «A feasibility study of solar PV-powered electric cars using an interdisciplinary modeling approach for the electricity balance, CO2 emissions, and economic aspects: The cases of The Netherlands, Norway, Brazil, and Australia», *Progress in Photovoltaics: Research and Applications*, vol. 28, n. 6, pagg. 517–532, 2020, doi: 10.1002/pip.3202.

[18] M. M. Gamil, T. Senjyu, H. Masrur, H. Takahashi, e M. E. Lotfy, «Controlled V2Gs and battery integration into residential microgrids: Economic and environmental impacts», *Energy Conversion and Management*, vol. 253, pag. 115171, feb. 2022, doi: 10.1016/j.enconman.2021.115171.

[19] T. Terlouw, T. AlSkaif, C. Bauer, e W. van Sark, «Multi-objective optimization of energy arbitrage in community energy storage systems using different battery technologies», Applied Energy, vol. 239, pagg. 356–372, 2019.

[20] A. Cabrera-Tobar, A. M. Pavan, N. Blasuttigh, G. Petrone, e G. Spagnuolo, «Real time Energy Management System of a photovoltaic based e-vehicle charging station using Explicit Model Predictive Control accounting for uncertainties», *Sustainable Energy, Grids and Networks*, pag. 100769, mag. 2022, doi: 10.1016/j.segan.2022.100769

[21] A. Bartolini, F. Carducci, C. B. Muñoz, e G. Comodi, «Energy storage and multi energy systems in local energy communities with high renewable energy penetration», *Renewable Energy*, vol. 159, pagg. 595–609, ott. 2020, doi: 10.1016/j.renene.2020.05.131.

[22] James B. Rawlings, David Q. Mayne, Moritz M. Diehl, "Model Predictive Control: Theory, Computation, and Design 2nd Edition", Nob Hill Publishing, 2020.

[23] Jiefeng Hu, Yinghao Shan, Josep M. Guerrero, Adrian Ioinovici, Ka Wing Chan, Jose Rodriguez, "Model predictive control of microgrids – An overview," Renewable and Sustainable Energy Reviews, Volume 136, 2021.

[24] Marcelo M. Morato, José Vergara-Dietrich, Eugene A. Esparcia, Joey D. Ocon, Julio E. Normey-Rico, "Assessing demand compliance and reliability in the Philippine off-grid islands with Model Predictive Control microgrid coordination," Renewable Energy, Volume 179, 2021, Pages 1271-1290.

[25] A. La Bella, S. Raimondi Cominesi, C. Sandroni and R. Scattolini, "Hierarchical Predictive Control of Microgrids in Islanded Operation," in *IEEE Transactions on Automation Science and Engineering*, vol. 14, no. 2, pp. 536-546, April 2017.

[26] A. La Bella, S. Negri, R. Scattolini and E. Tironi, "A Two-Layer Control Architecture for Islanded AC Microgrids with Storage Devices," *2018 IEEE Conference on Control Technology and Applications (CCTA)*, Copenhagen, 2018, pp. 1421-1426.

[27] P. Nahata, A. La Bella, R. Scattolini and G. Ferrari-Trecate, "Hierarchical Control in Islanded DC Microgrids With Flexible Structures," in *IEEE Transactions on Control Systems Technology*, vol. 29, no. 6, pp. 2379-2392, Nov. 2021.

[28] J.M. Manzano, J.R. Salvador, J.B. Romaine, L. Alvarado-Barrios, "Economic predictive control for isolated microgrids based on real world demand/renewable energy data and forecast errors," Renewable Energy, Volume 194, 2022, Pages 647-658.

[29] Chuanshen Wu, Shan Gao, Yu Liu, Tiancheng E. Song, Haiteng Han, "A model predictive control approach in microgrid considering multi-uncertainty of electric vehicles," Renewable Energy, Volume 163, 2021, Pages 1385-1396.

[30] Simone Negri, Federico Giani, Alessandro Massi Pavan, Adel Mellit, Enrico Tironi, "MPC-based control for a stand-alone LVDC microgrid for rural electrification," *in Sustainable Energy, Grids and Networks*, Volume 32, 2022.

[31] A. Mellit, A. Massi Pavan, V. Lughi, "Deep learning neural networks for short-term photovoltaic power forecasting," Renewable Energy, Volume 172, 2021, Pages 276-288.

[32] Jiaqi Qu, Zheng Qian, Yan Pei, "Day-ahead hourly photovoltaic power forecasting using attention-based CNN-LSTM neural network embedded with multiple relevant and target variables prediction pattern," Energy, Volume 232, 2021.

[33] Deniz Korkmaz, "SolarNet: A hybrid reliable model based on convolutional neural network and variational mode decomposition for hourly photovoltaic power forecasting," Applied Energy, Volume 300, 2021.

[34] A. Jędrzejewski, J. Lago, G. Marcjasz and R. Weron, "Electricity Price Forecasting: The Dawn of Machine Learning," in *IEEE Power and Energy Magazine*, vol. 20, no. 3, pp. 24-31, May-June 2022.

[35] M. Cerjan, I. Krželj, M. Vidak and M. Delimar, "A literature review with statistical analysis of electricity price forecasting methods," *Eurocon 2013*, 2013, pp. 756-763.

[36] Wendong Yang, Shaolong Sun, Yan Hao, Shouyang Wang, "A novel machine learning-based electricity price forecasting model based on optimal model selection strategy," *Energy*, Volume 238, Part C, 2022.

[37] Léonard Tschora, Erwan Pierre, Marc Plantevit, Céline Robardet, "Electricity price forecasting on the day-ahead market using machine learning," *Applied Energy*, Volume 313, 2022.

[38] Gholamreza Memarzadeh, Farshid Keynia, "Short-term electricity load and price forecasting by a new optimal LSTM-NN based prediction algorithm," *Electric Power Systems Research*, Volume 192, 2021.

[39] Fermín Rodríguez, Alice Fleetwood, Ainhoa Galarza, Luis Fontán, "Predicting solar energy generation through artificial neural networks using weather forecasts for microgrid control," Renewable Energy, Volume 126, 2018, Pages 855-864.

[40] Mario A. Tovar Rosas, Miguel Robles Pérez, E. Rafael Martínez Pérez, "Itineraries for charging and discharging a BESS using energy predictions based on a CNN-LSTM neural network model in BCS, Mexico,"! Renewable Energy, Volume 188, 2022, Pages 1141-1165.

[41] Donghun Lee, Kwanho Kim, "PV power prediction in a peak zone using recurrent neural networks in the absence of future meteorological information," Renewable Energy, Volume 173, 2021, Pages 1098-1110.

[42] Ali Agga, Ahmed Abbou, Moussa Labbadi, Yassine El Houm, "Short-term self consumption PV plant power production forecasts based on hybrid CNN-LSTM, ConvLSTM models," Renewable Energy, Volume 177, 2021, Pages 101-112.

[43] Kacem Gairaa, Cyril Voyant, Gilles Notton, Saïd Benkaciali, Mawloud Guermoui, "Contribution of ordinal variables to short-term global solar irradiation forecasting for sites with low variabilities," Renewable Energy, Volume 183, 2022, Pages 890-902.

[44] Xiaoqiao Huang, Qiong Li, Yonghang Tai, Zaiqing Chen, Jun Zhang, Junsheng Shi, Bixuan Gao, Wuming Liu, "Hybrid deep neural model for hourly solar irradiance forecasting," Renewable Energy, Volume 171, 2021, Pages 1041-1060.

[45] Neeraj Dhanraj Bokde, Bo Tranberg, Gorm Bruun Andresen, "Short-term CO2 emissions forecasting based on decomposition approaches and its impact on electricity market scheduling," *Applied Energy*, Volume 281, 2021.

[46] N. D. Pflugradt, «Modellierung von Wasser und Energieverbräuchen in Haushalten», 2016.

[47] https://www.loadprofilegenerator.de/

[48] A. de Almeida *et al.*, *E4 - Energy Efficient Elevators and Escalators (Technical Report)*. 2010. doi: 10.13140/2.1.2391.8400.

[49] PVGIS, https://ec.europa.eu/jrc/en/pvgis

[50] European Network of Transmission System Operators for Electricity - https://www.entsoe.eu/

[51] A. Caputo, «Fattori di emissione atmosferica di gas a effetto serra nel settore elettrico nazionale e nei principali Paesi Europei», ISPRA, 317/2020, 2020.

[52] Gli schemi di Autoconsumo Collettivo e le Comunità dell'Energia - https://dossierse.it/17-2020-gli-schemi-di-autoconsumo-collettivo-e-le-comunita-dellenergia

[53] Gurobi Optimizer, https://www.gurobi.com/

[54] IBM Cplex Optimizer, https://www.ibm.com/it-it/analytics/cplex-optimizer

[55] Yalmip Toolbox, https://yalmip.github.io/

[56] Sinha N.K., and Gupta M.M, 2000 soft computing and intelligent systems: Theory and application, Academic Press, USA.

[57] Hecht-Nielsen, R., 1992. Theory of the backpropagation neural network. In Neural networks for perception (pp. 65-93). Academic Press.

[58] Moré, J.J., 1978. The Levenberg-Marquardt algorithm: implementation and theory. In Numerical analysis (pp. 105-116). Springer, Berlin, Heidelberg.

[59] Sivanandam, S.N. Sumathi S., and Deepa, S.N., 2006. Introduction to neural networks using Matlab 6.0. McGraw-Hill Education, New Delphi.

[60] Ilaria Bendato, Andrea Bonfiglio, Massimo Brignone, Federico Delfino, Fabio Pampararo, Renato Procopio, "A real-time Energy Management System for the integration of economical aspects and system operator requirements: Definition and validation," Renewable Energy, Volume 102, Part B, 2017, Pages 406-416.

[61] https://www.arera.it/it/dati/condec.htm

[62] A. M. Pavan, V. Lughi and M. Scorrano, "Total Cost of Ownership of electric vehicles using energy from a renewable-based microgrid," 2019 IEEE Milan PowerTech, 2019, pp. 1-6.

[63] Domenico Mazzeo, "Nocturnal electric vehicle charging interacting with a residential photovoltaic-battery system: a 3E (energy, economic and environmental) analysis," Energy, Volume 168, 2019, Pages 310-331.